

## Article

# *NTH2* 1271\_1272delTA Gene Disruption Results in Salt Tolerance in *Saccharomyces cerevisiae*

Alejandro Hernández-Soto <sup>1,\*</sup> , José Pablo Delgado-Navarro <sup>2</sup>, Miguel Benavides-Acevedo <sup>3</sup> , Sergio A. Paniagua <sup>4</sup> and Andres Gatica-Arias <sup>3,5,6</sup> 

- <sup>1</sup> Doctorado en Ciencias Naturales para el Desarrollo (DOCINADE), Instituto Tecnológico de Costa Rica, Universidad Nacional, Universidad Estatal a Distancia, Cartago P.O. Box 159-7050, Costa Rica
  - <sup>2</sup> Costa Rica Institute of Technology, Biology School, Biotechnology Research Center (CIB), Cartago P.O. Box 159-7050, Costa Rica; jp2996@hotmail.com
  - <sup>3</sup> Laboratory of Plant Biotechnology, School of Biology, University of Costa Rica, San José P.O. Box 11501-2060, Costa Rica; miguel.benavides@ucr.ac.cr (M.B.-A.); andres.gatica@ucr.ac.cr (A.G.-A.)
  - <sup>4</sup> Centro Nacional de Alta Tecnología CeNAT, Laboratorio Nacional de Nanotecnología LANOTEC, San José P.O. Box 1174-1200, Costa Rica; sergian@gmail.com
  - <sup>5</sup> Research Center in Cellular and Molecular Biology (CIBCM), University of Costa Rica, San José P.O. Box 11501-2060, Costa Rica
  - <sup>6</sup> Programa de Posgrado en Biología (PPB), School of Biology, University of Costa Rica, San José P.O. Box 11501-2060, Costa Rica
- \* Correspondence: alhernandez@itcr.ac.cr



**Citation:** Hernández-Soto, A.; Delgado-Navarro, J.P.; Benavides-Acevedo, M.; Paniagua, S.A.; Gatica-Arias, A. *NTH2* 1271\_1272delTA Gene Disruption Results in Salt Tolerance in *Saccharomyces cerevisiae*. *Fermentation* **2022**, *8*, 166. <https://doi.org/10.3390/fermentation8040166>

Academic Editor:  
Alessandro Robertiello

Received: 17 January 2022

Accepted: 30 March 2022

Published: 5 April 2022

**Publisher's Note:** MDPI stays neutral with regard to jurisdictional claims in published maps and institutional affiliations.



**Copyright:** © 2022 by the authors. Licensee MDPI, Basel, Switzerland. This article is an open access article distributed under the terms and conditions of the Creative Commons Attribution (CC BY) license (<https://creativecommons.org/licenses/by/4.0/>).

**Abstract:** Trehalose is a common energy reservoir, and its accumulation results in osmotic protection. This sugar can accumulate through its synthesis or slow degradation of the reservoir by trehalase enzymes. *Saccharomyces cerevisiae* contains two neutral trehalases, *NTH1* and *NTH2*, responsible for 75% and 25% of the enzymatic metabolism. We were interested in the loss-of-function of both enzymes with CRISPR/Cas9. The later *NTH2* was of great importance since it is responsible for minor metabolic degradation of this sugar. It was believed that losing its functionality results in limited osmotic protection. We constructed an osmotolerant superior yeast capable of growing in 0.85 M NaCl after independent *nth2* 1271\_1272delTA mutation by CRISPR/Cas9 technology, compared with *nth1* 893\_894insT and wild type. We suggest that this yeast model could give clues to breeding commercial yeast resulting in non-GMO salinity-tolerant strains.

**Keywords:** mutation; precision biotechnology; stress tolerance; osmotolerance

## 1. Introduction

Trehalose ( $\alpha$ -D-glucopyranosyl- $\alpha$ -D-glucopyranoside) is a stress-tolerance-related sugar [1]. This nonreductive disaccharide, composed of two molecules of D-glucose, is also common in the metabolism of bacteria, fungi, plants, and some invertebrate animals [2–4]. Trehalose protects against structural disorders during water removal. It has been suggested that the hydroxyl groups of trehalose form hydrogen bonds with polar lipids and proteins instead of water, protecting these hydroxyl groups from structural disorder during water removal [5]. Trehalose can also work indirectly by stabilizing heat shock proteins during the refolding of damaged proteins [6]. Trehalose acts as a cryoprotectant to avoid aggregation by stabilizing proteins in a chaperone-like manner [5,7–10].

The intracellular accumulation of this disaccharide is due to the trehalose synthesis complex: *TPS1*, *TPS2*, *TPS3*, and *TSL1* [11]. However, the *NTH1*, *NTH2*, and *ATH1* genes are responsible for degrading trehalose and are also positively regulated under stress conditions, creating a metabolic cycle of carbohydrate regulation whose understanding is still controversial [12,13]. A high intracellular concentration of this molecule results in protecting the structures of biomolecules and the blockage of proteases while allowing

better recovery under stress [12,14,15]. Otherwise, the excessive accumulation of trehalose obstructs the active transport of glucose and inhibits growth in yeast [1,16].

*Saccharomyces cerevisiae* was used as our model organism for a proof-of-concept study to achieve salt-tolerant phenotypic traits using CRISPR/Cas9 editing and independent disruption of *NTH2* compared to wild type and *NTH1* disruption. A CRISPR-derived mutant is considered conventional in many legal frameworks like Brazil, allowing further breeding of commercial strains with no regulatory constraints [17]. We avoided other techniques such as homolog recombination because it could result in a genetically modified organism (GMO) limiting its industrial use.

Three enzymes are responsible for trehalose degradation in yeast: *NTH1* and *NTH2* are cytosolic neutral pH orthologs, while the third ortholog, *ATH1*, is a vacuolar acid pH enzyme [12,18]. The neutral trehalases *NTH1* and *NTH2* are responsible for 75% and 25% of the intracellular hydrolysis of carbohydrates, respectively [19]. We selected salt tolerance since yeast tends to decrease in viability under sodium chloride osmotic stress conditions. The viability of *S. boulardii* decreased at 0.4 M NaCl [20], and *S. cerevisiae* showed decreased viability at 0.68 M NaCl (4% *m/v*) [21].

Previous research on trehalases has dismissed the importance of *NTH2* because of its low expression and has instead focused on *NTH1* [7,22,23]. It was proposed that *NTH1* is the only protein that performs hydrolysis activity but that it works together with *NTH2* for hydrolysis recovery after exposure to high temperatures [14,15,24]. The *NTH1* and *NTH2* genes encode functional trehalases, with *NTH2* playing a protagonist role in the stationary phase [18]. It has also been proposed that eliminating the *NTH1* gene and overexpressing *tps1* (trehalose-6-phosphate synthase) increases trehalose and improves survival in high ethanol concentrations [7,22]. The deletion of all three of these enzymes results in intracellular trehalose accumulation and improved salt stress recovery [12]. The triple deletion of trehalases in yeast leads to tolerance of high concentrations of ethanol and high temperatures and higher viability after freezing [25]. Eliminating the *NTH1* and *NTH2* genes together in *S. cerevisiae* results in up to 180 days of resistance under stress conditions [26]. However, it seemed that eliminating the *NTH2* gene resulted in no salt tolerance [13]. Finally, accumulating trehalose resulting from neutral trehalases being knocked out then affects the growth of yeast [16].

In this article, we report a CRISPR/Cas9-specific *NTH2* 1271\_1272~~TA~~ disruption in *S. cerevisiae* that results in the capacity of the yeast to grow in 0.85 M NaCl and tolerate 1.2 M NaCl in comparison with non-mutant and mutant *NTH1* 893\_894~~insT~~ strains. We propose that disrupting *NTH2* alone with our design in yeast can trigger stress tolerance, although the mechanism remains unknown. To our knowledge, there is no formal report linking the disruption of *NTH2* alone to stress tolerance in *S. cerevisiae*. The knowledge generated herein is potentially valuable to improve industrial yeast or serve as a model to develop osmotic stress tolerance in other organisms using a similar rationale.

## 2. Materials and Methods

### 2.1. The Strain, Medium, and Growth Conditions

*S. cerevisiae* CEN.PK2-1C (*MATa*; *his3D1*; *leu2-3\_112*; *ura3-52*; *trp1-289*; *MAL2-8c*; *SUC2*) was used for all experiments. Cultures were grown in YPD medium (2% yeast extract, 1% peptone, and 2% dextrose), YPD agar (2% yeast extract, 1% peptone, 2% dextrose, and 2.2% agar) or YPAD (2% yeast extract, 1% peptone, 2% dextrose, and 40 mg/L adenine hemisulfate) at 30 °C at 200 rpm on an orbital shaker (Digisystem Laboratory Instruments Inc., New Taipei City, Taiwan). All reagents were purchased from Thermo Fisher Scientific® (Thermo Fisher, Carlsbad, CA, USA).

### 2.2. Preparation of the CRISPR Plasmid

Plasmid *bRA89*, containing *Streptococcus pyogenes* Cas9, a single guide scaffold, and hygromycin B resistance, was purchased from Addgene [27]. The single guide targeting the gene *NTH1* (YDR001C, strain ATCC 204508/S288c) and *NTH2* (YBR001C, strain

R64-1-1.80) was designed using the CRISPRdirect Platform [28]. Recognition of the single guide insertion for the *NTH2* gene (5'-TGCTATTAAAGAATATAAAG [AGG]-3') and *NTH1* (5'-GGTTACCCCTTATGCTGTTCC [TGG]-3') were cloned into bRA89 at Genscript, just below the RNA scaffold section, using *BpI*I restriction sites. Sanger sequencing confirmed the insertion of the single guide section next to the 5' end of the RNA scaffold. More details are provided in the Supplementary Materials (Figures S1 and S2).

### 2.3. *S. cerevisiae* Competent Cell Preparation and Transformation

Competent cells were prepared and transformed using the lithium acetate (LiAc) method with the following modifications [29]. An aliquot of approximately  $1 \times 10^7$  cells/mL (16 h culture) was inoculated in 50 mL of YPD medium and incubated until reaching an OD (600 nm) of 0.5. Then, the biomass was harvested by centrifugation (4000 rpm) for 10 min at room temperature, washed twice in 10 mL of sterile distilled water, and resuspended in 1.5 mL of sterile lithium acetate buffer (1 volume of TE 10X buffer, pH 7.5; 1 volume of 1 M LiAc, pH 7.5 and 8 volumes of distilled water). Freshly prepared competent yeast cells (200  $\mu$ L) were mixed with 1  $\mu$ g of the final plasmid and combined with 200  $\mu$ g of denatured Salmon Sperm DNA (Thermo Fisher, Carlsbad, CA, USA) and 1 mL of fresh PEG buffer (8 volumes of PEG 3350 50% and 1 volume of TE 10X buffer, pH 7.5; 1 volume of 1 M LiAc 10X, pH 7.5). The solution was incubated at 150 rpm for 30 min at 25 °C and then heated to 42 °C for exactly 15 min. Subsequently, the solution was resuspended in 200  $\mu$ L of YPAD medium and incubated for another 45 min at 25 °C. Finally, the cells were cultured on YPD agar plates supplemented with hygromycin B Phytotechnology Laboratories® (Shawnee Mission, KS, USA) at 500  $\mu$ g mL<sup>-1</sup> for 72 h at 28 °C in an incubator.

### 2.4. Selection and Sequencing Confirmation of Mutants

Thirty (30) randomly selected strains were grown on YPD overnight media. Subsequently, the manufacturer's instructions obtained genomic DNA using the ReliaPrep™ gDNA Tissue Miniprep System (Promega, Madison, WI, USA). Specific primers flanking the target sgRNA site of the *NTH2* gene were designed and named *nth2f*: 5'-GCAAGAGG TATGGTGGAGCA-3' and *nth2r*: 5'-TTCAGCTAGCTCCTCCCAGT-3' (Tm 55 °C; 539 bp); while *NTH1* primers flanking the target sgRNA site were also designed and named *nth1f*: 5'-ACCCCCGGTTTACTAGCATTG-3' and *nth1r*: 5'-TAAGGTAACGCCGTGTTTCGA-3' (Tm 55 °C; 528 bp). Sanger sequencing of PCR products was performed in MacroGen at Rockville, MD, USA, to confirm the mutation and absence of off-targets. We selected two isolates with the same mutation on the *NTH2*-disrupted gene and intact *NTH1* gene, named *nth2 1271\_1272delTA*. Similarly, we selected two isolates with the *NTH1*-disrupted gene and intact *NTH2* gene, named *nth1 893\_894insT*.

### 2.5. *nth1 893\_894insT* and *nth2 1271\_1272delTA* Strain Phenotypes

The methylene blue staining technique allowed examination of the viability of the wild-type and mutated yeast strains in 0.85 M NaCl versus the control (0 M NaCl) on Potato Dextrose (PD) (20% Potato, 2% dextrose) for 48 h at 28 °C. Growth curves of the samples were generated with 0 and 0.85 M NaCl in the YPD medium. The test was carried out with a SPECTROstarNANO plate reader from BMG LABTECH at 200 rpm and 30 °C for 24 h, with four repetitions per variant. The growth curve comparisons resulted from *T*-test analysis with and without saline stress conditions of the wild-type and mutated strains. The comparison also consisted of serial dilutions on agar PD plate-based comparison after two weeks of growth under stress (0.85 M and 1.2 M NaCl). Trehalose content was extracted following the protocol described by Divate et al. [22] with the following variations. The cells were grown after 0.85 M NaCl versus the control (0 M NaCl) on PD for 48 h at 28 °C, collected by centrifugation at 7000 × *g* for 5 min and dried at 100 °C for 12 h. A pellet of 50 mg was mixed with 1 mL ethanol (99.5%) and incubated in a boiling water bath for 1 h. HPLC-RID determined the content, P-SA-MQ-006 provided by CITA-UCR, as follows: The ethanolic extract was centrifuged and filtered through a 0.20  $\mu$ m regenerated cellulose

micropore (17761-Q, Minisart-RC15<sup>®</sup>, Sartorius AG, Göttingen, Germany), the filtrate was collected in a 2 mL vial for HPLC. AC Chromatographic separation was performed using Agilent Technologies 1260 Infinity liquid chromatograph equipped with Suplecogel 8Ca high resolution column (300 mm × 7.8 mm, 8 μm, PN 59247-U), quaternary pump (G1311B), column compartment (G1316A), automatic liquid sampling module (ALS, G7129A) and refractive index detector (G1362A) (Agilent Technologies, Santa Clara, CA, USA). The mobile phase consisted of ultrapure water (type I, 0.055 μS cm<sup>-1</sup> at 25 °C, 5 μg L<sup>-1</sup> TOC) obtained using A10 Milli-Q Advantage and Elix 35 purification system (Merck KgaA, Darmstadt, Germany). Solvent flow, column compartment temperature, detector cell temperature, and injection volume were constant during the elution at 0.40 mL min<sup>-1</sup>, 80 °C, 40 °C, and 10 μL, respectively. The area under the curve (AUC) of the trehalose signal in the samples was interpolated in the calibration curve of the certified reference standard (Sigma-Aldrich, PHR1344-500 mg), in a concentration range of 0.025 to 0.25 g/100mL.

### 2.6. Statistical Software

Minitab v.19.1.1 supported statistical analysis and RStudio v.1.1.423 was used for visualization.

### 2.7. Scanning Electron Microscopy (SEM)

Wild-type and mutated yeast grown in 0.00 and 0.85 M NaCl and fixed with Karnovsky fixative (2.5% *w/v* of glutaraldehyde, 0.1 M of paraformaldehyde in phosphate buffer pH 7.4, during 48 h at 4 °C) were mounted on carbon tape and sputtered with gold using a Denton Vacuum Desk V sputter system at 20 mA for 300 s. Images were taken using a JSM-6390LV (JEOL, Tokyo, Japan) scanning electron microscope with an accelerating voltage of 15 kV under high vacuum. Scanning electron microscopy images at different resolutions of the wild-type and *NTH2*-mutated yeasts and subsequent cell area calculations were analyzed with ImageJ version 1.52p.

### 2.8. Transmission Electron Microscopy (TEM)

Wild-type and mutated yeast grown with and without NaCl were treated with Karnovsky fixative for six days. The yeast was then centrifuged at 3000 rpm for 5 min and rinsed with 0.1 M phosphate buffer solution (pH 7.2) for three 15 min wash/centrifugation cycles. The yeast samples were then stirred for one hour in 2% *w/v* OsO<sub>4</sub> in 0.1 M phosphate buffer solution, followed by three wash cycles as per the previous step but with type 3 water instead of buffer. The yeasts were finally isolated via centrifugation at 3000 rpm for 10 min and subsequently embedded in a solution of agar/agarose 4% *w/v* in a hot water bath (50 °C). After cooling to 37 °C, one drop of the solution was added to an Eppendorf tube containing 100 μL of the yeast sediment and mixed thoroughly. After cooling, the solids were removed and cut into 3 mm<sup>3</sup> segments. Dehydration was performed by rinsing in an ascending gradient of acetone (30% to 100% *v/v*) followed by infiltration with Spurr resin: acetone 50:50 overnight and three successive infiltrations with pure Spurr resin for two hours each. The resulting solids were transferred to BEEM embedding capsules. Polymerization was achieved in an oven at 70 °C for 24 h. Ultrafine segments (approximately 70 nm) were cut with a Leica EM UC7 ultramicrotome with a diamond knife and supported on Cu TEM grids (200 mesh). The sections were stained with 4% *m/v* uranyl acetate in 50% *v/v* ethanol for 15 min and washed five times in DI water, followed by soaking for 10 min in Reynold's stain and rinsing five times in water. Once dry, the grids were mounted in a JEOL JEM 2011 TEM and observed at 120 kV at magnifications of 3000–20,000×.

## 3. Results

### 3.1. Confirmation of *NTH1-NTH2* Gene-Mutated Cells

*NTH1* and *NTH2* disruption were confirmed in the randomly selected strains. We selected two isolates of *NTH2* mutant strains named *nth2* 1271\_1272*delTA* containing the same mutation, a deletion of two bases, TA, located at positions 1271-1272, three bases

downstream from the PAM site expected. A PCR of the target sequence (Figure 1A) and Sanger sequencing confirmed that the deletion was present in only the strains treated with the CRISPR/Cas9 technique directed through the single guide RNA complementary to section 1258 to 1276 of the *NTH2* compared with the chromosome 2 sequence. Sequencing also confirmed that the open reading frame disruption results from forming the TAA triplet in the respective open reading frame, creating a stop codon at amino acid 424 (Figure 1B). Additionally, the integrity of the *NTH1* gene was verified in the *NTH2*-mutated strain by PCR and sequencing of the specific mutation zone. The *S. cerevisiae* *NTH1* gene was not altered due to CRISPR/Cas9 genome editing in the strain *nth2 1271\_1272delTA*.

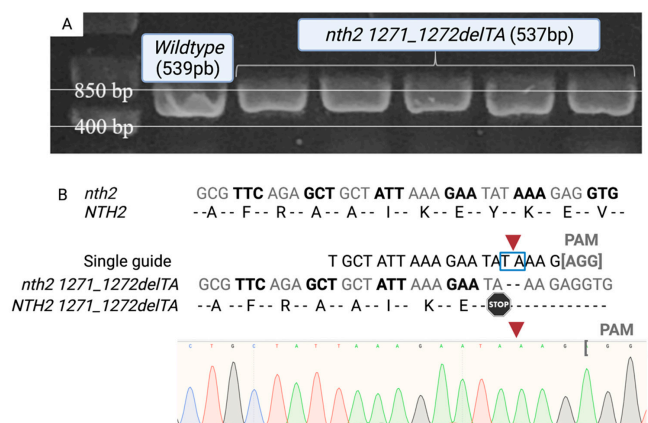


**Figure 1.** Confirmation of *NTH2* gene disruption in *S. cerevisiae* by CRISPR/Cas9. (A). Amplification of the segment containing the expected mutation site on a 1% *m/v* agarose gel; (B). Sequencing of the *S. cerevisiae* *NTH2* gene. In the box, it can be observed how the deletion 1271\_1272delTA caused the Y424X mutation in the *nth2 1271\_1272delTA* strain. Image created with [BioRender.com](https://www.biorender.com) (accessed on 30 March 2022).

The *NTH1* mutant strains named *nth1 893\_894insT*, consisted of three strains containing an insertion of one base, T, located at a position three bases downstream from the PAM site, as expected. The insertion results in disruption of the open reading frame three triplets downstream TAG, resulting in a truncated 301 AA protein with SWW\* instead of PGGR (Figure 2).

Mutation on the *NTH1* and *NTH2* genes showed disruption and absence of the active sites for a putative first ORF protein translated, specifically amino acid residues D478, E674 for *NTH1*, and D507 and E703 for *NTH2*. The *nth2 1271\_1272delTA* may produce a small truncated 423 amino acid protein instead of the complete enzyme, lacking biochemical function. Similarly, the insertion in *NTH1* results in a knockout of three triplets downstream of TAG, resulting in a truncated 301 AA with no disaccharide binding site. The truncated sequence of mutants *nth1 893\_894insT* and *nth2 1271\_1272delTA* may still contain the Ca<sup>2+</sup> binding domain if the three-dimensional conformation is unchanged.

When comparing the resulting putative Open Reading Frames, we noted that phosphorylation activation of the enzymes remains in the amino terminal that corresponds to the first disrupted ORF of both *nth1 893\_894insT* and *nth2 1271\_1272delTA*. A putative, predicted second ORF corresponding to the carboxyterminal end is different for each mutant. In the case of *nth1 893\_894insT*, the second ORF may have all the binding sites (R302, N346, E424, R473, G476), active sites (D507, E703), and substrate binding sites (338-339WD, 384-386RSQ) in the second ORF. In the case of *nth2 1271\_1272delTA*, the sites may be spliced by having one binding site (G505) and the active sites in the second ORF (D478, E674), but most binding sites (R331, N375, R384) and all substrate binding sites (309-310WD, 355-357RSQ) in the first ORF (Table 1).

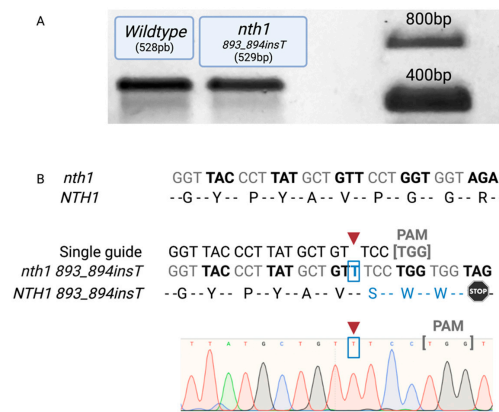


**Figure 2.** Confirmation of *NTH1* gene disruption in *S. cerevisiae* by CRISPR/Cas9. (A). Amplification of the segment containing the expected mutation site on a 1% *m/v* agarose gel; (B). Sequencing of the *S. cerevisiae* *NTH1* gene revealed the insertion of a T in position 893 resulting in a truncated 301 AA protein with SWW\* instead of PGGR. Image created with [BioRender.com](https://BioRender.com) (accessed on 30 March 2022).

**Table 1.** Predicted Open Reading Frames (ORF) of mutants in comparison with the wild-type *NTH1* and *NTH2* genes.

Gene	Open Reading Frames
<i>NTH1 wild type</i>	MSQVNTSQGPVAQGRQRRLSSLSSEFNDFPFSNAEVYYPPTDPRKQKQAK PAKINRTRTMSVFDNVSPFKKTGFGKLGKQTRRGSSEDDTYSSSQGNRRFF IEDVDKTLNELLAEDTDKNYQITIEDTGPKVLKVGTSANSYGYKHINIR GTYMLSNLLQELTIAKSFGRHQIFLDEARINENPVNRLSRLINTQFWNS LTRRVDLNNVGEIAKDTKIDTPGAKNPRIYVPYDCPEQYEFYVQASQM HPSLKLEVEYL PPKITA EYVKS VNDTPG LLALAMEEHFNPSTGEKTLIG YPYAVPGGRFNELYGWDSYMMALGLLEANKTDVARGMVEHFIFEINHY GKILNANRSYLLCRSQPPFLTEMALVVFKKLGGRSNPDAVDLLKRAFQA SIKEYKTVWTASPR LDPETGLSRYHPNGLGIPPETESDHFDTVLLPYASK HGVTLDEFKQLYNDGKIKEPKLDEFFLHDRGVRESGH DTTYRFEGVCA YLATIDLNSLLYKYEIDIADFIKEFCDDKYEDPLDHSITTSAMWKEMAK IRQEKITKYMWDDESGFFDYNTKIKHRTSYESATTFWALWAGLATKE QAQKMVEKALPKLEMLGGLAACTERSRGPISIRPIRQWDYPFGWAP HQILAWEGLRSYGYLTVTNRLAYRWLFMMTKAFVDYNGIVVEKYDVT RGTDPHRVEAEYGNQGADFKGAATEFGWVNASYILGLKYMNSHAR RALGACIPPISFFSLRPQERNLYGL
<i>nth1 893_894insT, ORF1</i>	MSQVNTSQGPVAQGRQRRLSSLSSEFNDFPFSNAEVYYPPTDPRKQKQAK PAKINRTRTMSVFDNVSPFKKTGFGKLGKQTRRGSSEDDTYSSSQGNRRFF IEDVDKTLNELLAEDTDKNYQITIEDTGPKVLKVGTSANSYGYKHINIR GTYMLSNLLQELTIAKSFGRHQIFLDEARINENPVNRLSRLINTQFWNS LTRRVDLNNVGEIAKDTKIDTPGAKNPRIYVPYDCPEQYEFYVQASQM HPSLKLEVEYL PPKITA EYVKS VNDTPG LLALAMEEHFNPSTGEKTLIG YPYAVSWW
<i>nth1 893_894insT, ORF2</i>	MLFPGGRFNELYGWDSYMMALGLLEANKTDVARGMVEHFIFEINHYG KILNANRSYLLCRSQPPFLTEMALVVFKKLGGRSNPDAVDLLKRAFQAS IKEYKTVWTASPR LDPETGLSRYHPNGLGIPPETESDHFDTVLLPYASK HGVTLDEFKQLYNDGKIKEPKLDEFFLHDRGVRESGH DTTYRFEGVCA YLATIDLNSLLYKYEIDIADFIKEFCDDKYEDPLDHSITTSAMWKEMAK IRQEKITKYMWDDESGFFDYNTKIKHRTSYESATTFWALWAGLATKE QAQKMVEKALPKLEMLGGLAACTERSRGPISIRPIRQWDYPFGWAP HQILAWEGLRSYGYLTVTNRLAYRWLFMMTKAFVDYNGIVVEKYDVT RGTDPHRVEAE YGNQGADFKGAATEFGWVNASYILGLKYMNSHAR RALGACIPPISFFSLRPQERNLYGL

**Table 1.** Cont.

Gene	Open Reading Frames
<i>NTH2 wild type</i>	MVDFLPKVTEINPPSEGNDGEDNIKPLSSGSEQRPLKEEGQQGRRHH <u>RRLSSMHEYFDPFSNAEVYGPITDPRKQSKIHRLNRTRTMSVFNKVS</u> FKNGMKDYTLKR <u>RGSEDD</u> SFLSSQGNRRFYIDNVDLALDELLASEDT KNHQITIEDTGPKVIKVG TANSNGFKHVNVRGTYMLS NLLQELTI AKS FGRHQIFLDEARINENPVDRLSRLITTQFWTSLRRVDLYNIAE IARDSK IDTPGAKNPRI YVPYNCPEQYEFYIQASQMNP SLKLEVEYLPKDITAEY VKSLNDTPGLLALAMEEHVNPSTGERSLVGYPYAVPGGR <u>RFNELYGWD</u> SYLMALGLIESNKVDVARGMVEHFIFEIDHYSKIL <u>NANRSYLLCRSQPP</u> FLTDMALLVFEK IGGKNNPNAIQLLKRAFRAAIKEYKEVWMS <u>SPRLD</u> SLTGLSCYHSDGIGIPPETEPDHFDTILLPYAEKYNVTLEKLR <u>LYNEGM</u> IKEPKLDAFFLHDRAVRES <u>SGH</u> DTTYRFEGVCAYLATIDLNS <u>LLYKYEK</u> IAFVIKEYFGNEYKDENDGTVDSEHWEELAE LRKTRINKYMWDEDS GFFFYNTK LKCRTSYESATTFWSLWAGLATEEQAKITVEKALPQLEML GGLVACTEKS RGPISIDRPIRQWDYPFGWAPHQILAWKGLSAYGYQV ATRLAYRWLYMITKSFVDYNGMVV <u>EKYDVTRGTD</u> PHRVD AEYGNQG ADFKGVATEGFGWVNTSYLLGLKYMNNHARRALAA <u>ACSPPLPFFNSL</u> PSEKKLYYL
<i>nth2</i> 1271_1272delTA, ORF1	MVDFLPKVTEINPPSEGNDGEDNIKPLSSGSEQRPLKEEGQQGRRHH <u>RRLSSMHEYFDPFSNAEVYGPITDPRKQSKIHRLNRTRTMSVFNKVS</u> DFKNMGKDYTLKR <u>RGSEDD</u> SFLSSQGNRRFYIDNVDLALDELLASEDT DKNHQITIEDTGPKVIKVG TANSNGFKHVNVRGTYMLS NLLQELTI AK SFGGRHQIFLDEARINENPVDRLSRLITTQFWTSLRRVDLYNIAE IARDS KIDTPGAKNPRIYVPYNCPEQYEFYIQASQMNP SLKLEVEYLPKDITAE YVKSNDTPGLLALAMEEHVNPSTGERSLVGYPYAVPGGR <u>RFNELYGWD</u> SYLMALGLIESNKVDVARGMVEHFIFEIDHYSKIL <u>NANRSYLLCRSQPP</u> FLTDMALLVFEKIGGKNNPNAIQLLKRAFRAAIKE
<i>nth2</i> 1271_1272delTA, ORF2	MSSPRLDSL TGLSCYHSDGIGIPPETEPDHFDTILLPYAEKYNVTLEKLR LYNEGMIKEPKLDAFFLHDRAVRE <u>SGH</u> DTTYRFEGVCAYLATIDLNS LLYKYEKDIAFV IKEYFGNEYKDENDGTVDSEHWEELAE LRKTRINK YMWDEDSGFFFYNTK LKCRTSYESATTFWSLWAGLATEEQAKITVEK ALPQLEMLGGLVACTEKS RGPISIDRPIRQWDYPFGWAPHQILAWKGL SAYGYQVATRLAYRWLYMITKSFVDYNGMVV <u>EKYDVTRGTD</u> PHRVD AEYGNQGA DFKGVATEGFGWVNTSYLLGLKYMNNHARRALAA <u>ACSP</u> PLPFFNSLKPSEKKLYYL

\* Binding site, *NTH1* in red R302, N346, E424, R473, G476; *NTH2* R331, N375, R384, G505; Active site in green *NTH1*: D478, E674; *NTH2*:D507, E703; Substrate binding underline *NTH1*: 338-339WD, 384-386RSQ; *NTH2* 309-310WD, 355-357RSQ; Phosphorylation site of activation *NTH1* S20, S21, S60, S83, *NTH2* R49, S52, R109, S112.

### 3.2. Behavior of the *nth2* 1271\_1272delTA Strain under Salinity Stress

The *nth2* 1271\_1272delTA strain has increased tolerance and can survive in high concentrations of NaCl (0.85 M NaCl). We noted that the *nth2* 1271\_1272delTA strains were slightly smaller than the control under the light microscopy, although we were not able to detect any statistical difference. We validated that the cells remained the same and had no statistical differences from the control under high osmolarity conditions and also with the scanning electron microscopy. Yeast dimensions were determined from the scanning electron microscopy images (Figure 3A). The sizes of the cells remained statistically and phenotypically identical to the wild-type strain and were not collapsed, although we noted that they were slightly smaller (Figure 3B).

The *nth2* 1271\_1272delTA strain cells were also not different under transmission electron microscopy analysis (data not shown). Organelles and structures such as vacuoles, nucleus, mitochondrion, cell membrane, and cell wall had no differences compared to the wild-type CEN.PK2-1C strain. We noted no organelle disruption nor structural changes in the tolerant strain (for more details check the Supplementary Materials).

The *nth2* 1271\_1272delTA strain was viable in a maximum concentration of 0.85 M NaCl and gave a standard growth curve and an average growth rate of  $0.2327 \pm 0.0057 \text{ h}^{-1}$  (Figure 4). When statistically analyzing the specific growth rates ( $p < 0.05$ ), the *nth2*

*1271\_1272delTA* strain under stress conditions had a growth rate of  $0.2179 \pm 0.0061 \text{ h}^{-1}$  and behaved in the same way as the wild-type strain under normal conditions  $0.2255 \pm 0.0037 \text{ h}^{-1}$ . The behavior of the wild-type strain in NaCl solution presented a significant decrease of  $0.1580 \pm 0.0009 \text{ h}^{-1}$ .

We expected a slight salt tolerance because of the neglected reported activity of *NTH2*. The latter was reasonable because the strain still had functional *NTH1* enzymes that metabolize trehalose. However, the data obtained showed that the *nth2 1271\_1272delTA* strains were superiorly tolerant. The *nth2 1271\_1272delTA* strains had an average growth curve in a 0.85 M NaCl liquid medium, with two isolates having the same mutation and behavior. Instead, the wild type had a slower growth curve (Figure 4).

We mutated the homolog gene *NTH1* resulting in *nth1 893\_894insT* strains to compare it with *nth2 1271\_1272delTA*. The *nth1 893\_894insT* strains showed no tolerance to 0.85 and 1.2 M NaCl when grown on agar plate-based comparison after two weeks (Figure 5). Growth on 0.85 M and 1.2 M was detected after three days for *nth2 1271\_1272delTA*, mutants but it took a week for the control and *nth1 893\_894insT* mutants. We could not detect *nth1 893\_894insT* salt tolerance when growing the mutant in 0.85 M NaCl liquid media (data not presented).

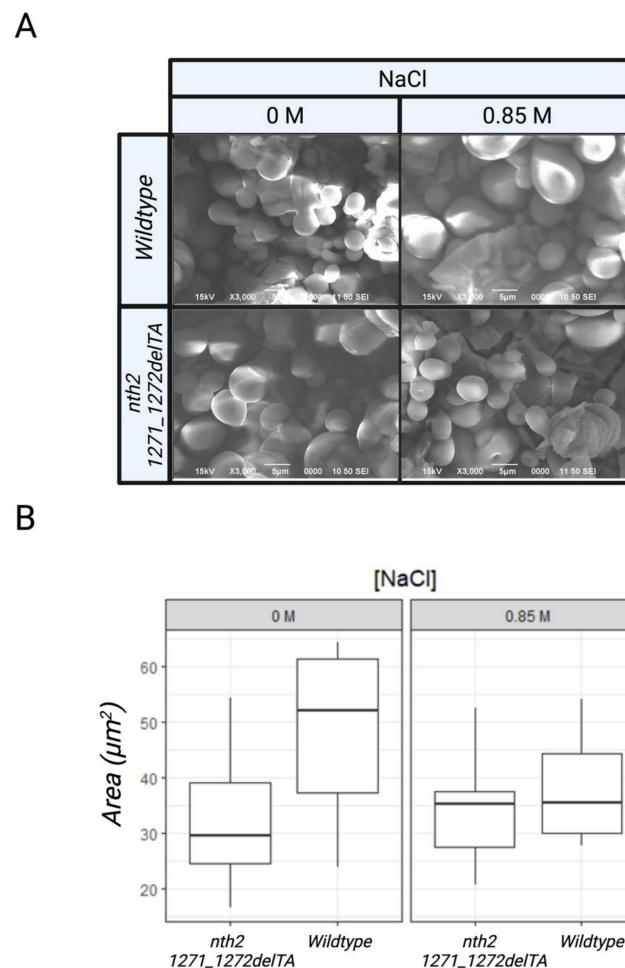


**Figure 3.** Analysis of the sizes of the wild-type and *nth2 1271\_1272delTA* yeasts. (A). Scanning electron microscopy views of the wild-type CEN.PK2-1C strain and mutated strain *nth2 1271\_1272delTA* grown in 0 and 0.85 M NaCl; (B). Box plots representing the sizes of the wild-type and *nth2 1271\_1272delTA* strains of yeast under nonstress and stress (NaCl) conditions. No significant difference was observed ( $p < 0.05$ ).

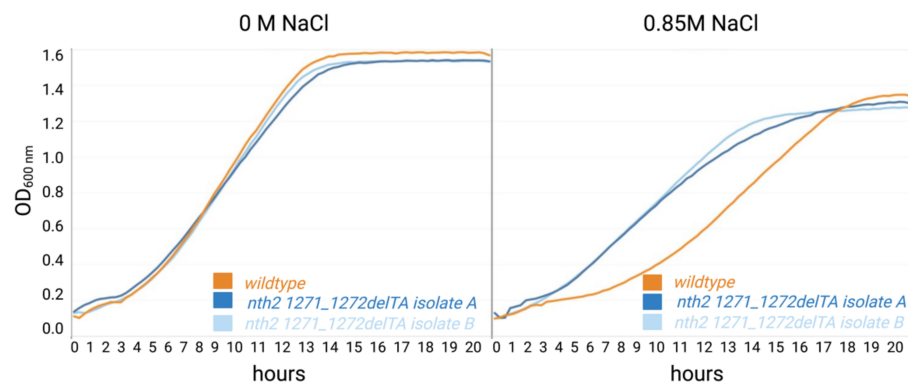


**Figure 4.** Growth curves of *S. cerevisiae* *nth2 1271\_1272delTA* strains in the presence and absence of osmotic stress (0.85 M NaCl) by indirect measurements of optical density at 600 nm after 20 h of growth under stress. The curve was built with the mean of four independent samples per hour for each condition. The growth rate was calculated for the wild type in non-stress conditions of  $0.2255 \pm 0.0037 \text{ h}^{-1}$  versus  $0.1580 \pm 0.0009 \text{ h}^{-1}$  in 0.85 M NaCl stress, and *nth2 1271\_1272delTA*  $0.2327 \pm 0.0057 \text{ h}^{-1}$  versus  $0.2179 \pm 0.0061 \text{ h}^{-1}$  in 0.85 M NaCl stress.

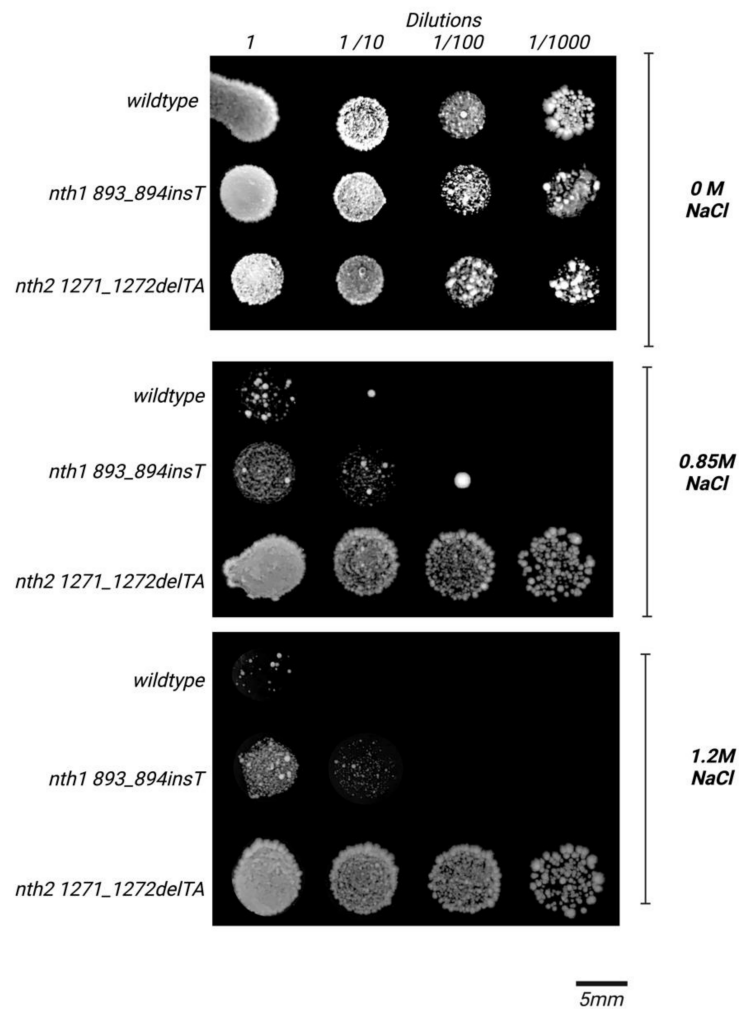


**Figure 5.** Agar plate comparison of yeast strains: *nth1 893\_894insT*, *nth2 1271\_1272delTA*, and wild-type after two weeks of growth under 0, 0.85 M and 1.2M NaCl stress. Note serial dilutions of yeast starting in  $OD_{600} = 1$ .

We noted no difference in the intracellular content of trehalose in *nth2 1271\_1272delTA* in comparison with the control in the stationary phase after 48h of growth with or without stress. However, in *nth1 893\_894insT*, the trehalose content was low with or without NaCl. (Table 2).

**Table 2.** Intracellular trehalose content of yeast cells under non-stress and stress conditions.

Strain <sup>1</sup>	Intracellular Content of Trehalose	
	0 M NaCl	0.85 M NaCl
<i>S. cerevisiae</i> CENPK2 (control)	(150 ± 22) mg 100 mL <sup>-1</sup>	(118 ± 18) mg/100 mL
<i>S. cerevisiae</i> CENPK2 <i>nth2 1271_1272delTA</i>	(139 ± 21) mg 100 mL <sup>-1</sup>	(107 ± 16) mg/100 mL
<i>S. cerevisiae</i> CENPK2 <i>nth1 893_894insT</i>	(34.8 ± 5.2) mg 100 mL <sup>-1</sup>	(33.8 ± 5.1) mg/100 mL

<sup>1</sup> All cells grew with the same conditions, trehalose content determined by HPLC.

#### 4. Discussion

The salinity tolerance of the *S. cerevisiae* strain CENPK2 increased when the *NTH2* gene was disrupted using CRISPR/Cas9-mediated genome editing compared with wild type and *NTH1* disruption. The *nth2 1271\_1272delTA* yeast strains grew in 0.85 M NaCl with no detectable changes in behavior other than stress tolerance. Although deletion of *NTH1* and *NTH1-NTH2* together was known to result in stress tolerance, to our knowledge, this is the first report of using the CRISPR/Cas9 technique to disrupt *NTH2* alone that results in remarkable stress tolerance, as confirmed by an automated measurement system. The result is similar to a predictive model suggesting such tolerance for *NTH2* kanMX4 deletion and a neglectable tolerance for *NTH1*-disrupted strains [30].

The use of CRISPR/Cas9 resulted in the expected specific mutations of the *S. cerevisiae* of both *NTH2* and *NTH1* independent genes, three bases downstream of the PAM section (NGG) with the *S. pyogenes* Cas9 enzyme [31,32]. In the case of *NTH2*, the double-strand break resulted in the deletion of two nucleotides after nonhomologous end joining (NHEJ), introducing the “TAA” stop codon in the respective open reading frame (Figure 1). The *nth2 1271\_1272delTA* strain had a deletion of two nucleotides, TA, located at positions 1271-1272, which resulted in a stop codon Y424X mutation of the *NTH2* gene; notably, no changes in the *NTH1* gene were observed. The anticipated tridimensional structure of the putative 423 amino acid Open Reading Frame (ORF) of *nth2 1271\_1272delTA* indicated that this modified enzyme should be inactive due to the absence of the active residues ASP507 and GLU703. Similarly, the *NTH1* mutant, *nth1 893\_894insT* contained an insertion of one T base three bases downstream of the PAM site as expected and resulted in an early stop codon three triplets downstream.

In this study, *nth2 1271\_1272delTA* strains remained viable and had better tolerance to 0.85 M NaCl than the wild-type and *nth1 893\_894insT* strains. The behavior and size of *S. cerevisiae nth2 1271\_1272delTA* did not change compared to the wild type and had normal variability depending on the generations and growth stage. Yeast tends to shrinkage and collapse in NaCl osmotic stress without plasmolysis, but its primary difference is in mitochondrial fragmentation [33]. We validate that *nth2 1271\_1272delTA* did not collapse under stress and was identical to the control with no stress and had no fragmentation of its organelles using transmission electron microscopy.

The *nth2 1271\_1272delTA* strain showed exponential growth under NaCl stress conditions ( $0.2179 \pm 0.0061 \text{ h}^{-1}$ ) very similar to the wild-type strain without the presence of the osmotic agent ( $0.2255 \pm 0.0037 \text{ h}^{-1}$ ). The results indicate that this mutation provides the yeast with a greater tolerance to saline conditions without significantly affecting its specific growth rate than the wild-type strain under salinity stress ( $0.1580 \pm 0.0009 \text{ h}^{-1}$ ).

Our data differ from previous reports that have proposed that eliminating the *NTH2* gene resulted in no salt tolerance [13]. However, the results are not comparable due to methodological differences of complete deletion of the gene versus a point mutation. We used 0.85 M NaCl stress from the beginning, an automatic growing system under constant

salt stress sampling every 15 min beginning at time 0 (Figure 4) and validated the tolerance in the semisolid plate (Figure 5). The growth rate is also not comparable with our control strain CENPK2 having half the growth rate in non-stress conditions of  $0.2255 \pm 0.0037 \text{ h}^{-1}$  versus  $0.1580 \pm 0.0009 \text{ h}^{-1}$  in stress, and *nth2 1271\_1272delTA*  $0.2327 \pm 0.0057 \text{ h}^{-1}$  versus  $0.2179 \pm 0.0061 \text{ h}^{-1}$  in stress. We believe that these automatic results and visual colony growth can capture the behavior of the mutation while reducing human error [33].

We foresee the disruption of *NTH2* to provide stress tolerance in an industrial strain, because undisrupted *NTH1* can provide the metabolic equilibrium as described next. *NTH1* and *NTH2* are required and regulated for fueling growth. *NTH1* is phosphorylated by Cdk1(S66) and PKA1 (S20, S21, S60, S83) to be activated, and is required for fueling biosynthesis during S, G2, and M [34]. *NTH2* contains an N terminal phosphorylation region (R49, S52, R109, S112) and is expressed at a high level in the stationary phase after glucose exhaustion [15]. *NTH2* and *NTH1* are downregulated at the exponential phase and have a higher expression at the stationary phase [19,35]. The presence of salinity stress causes trehalose accumulation in *S. cerevisiae* and higher ethanol osmotolerance [13,25]. Heat stress (40°C), CuSO<sub>4</sub>, NaAsO<sub>2</sub>, H<sub>2</sub>O<sub>2</sub>, cycloheximide (CHX) but not NaCl (1.5 M) trigger the expression of *NTH1* and, in practice, its disruption is unrequired for salt tolerance [36]. It is also known that strains with *NTH2* disruption, previously named YBR0106, grow normally in YEP glycerol and were associated with increased sensitivity against heat shock at 50 °C [14], while  $\Delta nth1$  grows poorly in YEP glycerol and cannot mobilize endogenous trehalose [24]. *NTH1* disruption may provide some stress tolerance but not related to NaCl, as previously reported [22]. However, disruption of *NTH1* may not be useful for industry because these mutants cannot hydrolyze trehalose after returning from a heat stress temperature of 40 °C to an average growth temperature of 30 °C [15].

We do not fully understand the tolerance since there were no detectable changes in trehalose in the stationary phase of *nth2 1271\_1272delTA* and the control as described next. We also did not note differences between the mutant *nth2 1271\_1272delTA* ( $107 \pm 16$ ) mg/100 mL and the control ( $118 \pm 18$  mg/100 mL) under stress conditions (0.85 M NaCl). Instead, *nth1 893\_894insT* mutants had a stable low concentration of trehalose in stress ( $33.8 \pm 5.1$  mg 100 mL<sup>-1</sup>) and non-stress ( $34.8 \pm 5.2$  mg 100 mL<sup>-1</sup>) conditions in comparison with the control in stress ( $118 \pm 18$  mg 100 mL<sup>-1</sup>) and non-stress conditions ( $150 \pm 22$  mg 100 mL<sup>-1</sup>). We expected no improvement of *nth1 893\_894insT* mutants in salt as previously reported [12]. In addition, no important change of intracellular trehalose was previously reported when *NTH2* is eliminated under osmotic NaCl stress [12,37]. However, in previous reports testing the relationship of *NTH1* and *NTH2* with pressure tolerance, the trehalose content was slightly high but not statistically different in  $\Delta nth2$  in stationary phase ( $\Delta nth2 = 316 \pm 66$  µg/mg of protein, wt =  $257 \pm 47$  µg mL<sup>-1</sup>,  $\Delta nth1 = 519 \pm 80$  µg mL<sup>-1</sup>). Notably,  $\Delta nth2$  acquired a barotolerance dismissed by the authors ( $\Delta nth2 = 5.0 \pm 2.0$ , wild type =  $3.4 \pm 1.0$ ,  $\Delta nth1 = 0.3 \pm 0.09$ ). Instead, the authors focused on  $\Delta nth1$  sensitivity although having a higher concentration of trehalose [37]. High trehalose concentration can protect from pressure but requires hydrolysis mediated by *NTH1* because it interferes with the reactivation of the cell [37,38]. A high trehalose concentration is insufficient for stress tolerance, but its correct use as an energy reservoir seems essential. Yeast cells subjected to 50 MPa of pressure results in the immediate induction of the *TPS1* gene (at 0', 5', 10', 15' was 2.41, 3.92, 4.15, 4.16) triggering trehalose synthesis, while *NTH1* and *NTH2* are induced primarily post-pressurization (at 0', 5', 10', 15' was *NTH1* = 0.41, 2.07, 2.78, 3.14; *NTH2* = 1.07, 2.23, 3.21, 3.73) [39].

*NTH2*-disrupted mutants can mobilize and use trehalose. Its mutation results in an increased acid trehalase activity [19], meaning that the metabolic stability of the strain is not compromised. In addition, no significant change in intracellular trehalose occurs when *NTH2* is eliminated under osmotic NaCl stress such as in our results [12,22]. The latter also means that trehalose negatively affects growth, for overaccumulation is unfeasible [16].

Interestingly, in *Cryptococcus neoformans*, the disruption of *NTH2* alone increased the survival ability of the yeast, but the deletion of *NTH1-NTH2* was negative for the

microorganism [40]. Similarly, a database of yeast mutants growth modeling completed with kanMX4 interrupting NTH2 in haploid BY4741 background predicts tolerance to salt stress, such as our results [30].

In our *NTH2* mutation model, an alternative explanation is that *nth2 1271\_1272delTA* translates the gene into two ORFs considering that yeast produces alternative ORFs [41–43]. In that case, the ORFs from *nth2 1271\_1272delTA* may not be active but may be able to bind the substrate. The protein fragments could transitorily protect trehalose from catabolism. The first ORF, containing binding sites R331, N375, R384, 309–10WD, and 355–357RSQ but not the active sites, could bind to the trehalose and protect the molecule from the enzymatic activity of *NTH1*.

Breeding industrial yeast can result in cost-effectiveness or reductions in fermentation. In the case of stress tolerance traits, yeast is constantly exposed to ethanol toxicity, oxidative stress, temperature stress, and osmotic stress, diminishing its capacity to produce ethanol [44,45]. Our data also show that the osmotic tolerance of the *nth2 1271\_1272delTA* disruption strain mediated by CRISPR is superior and could represent a solution for the fermentation industry without compromising its metabolism, phenotype, or behavior [46,47].

## 5. Conclusions

The *S. cerevisiae* *NTH2* gene was disrupted with the CRISPR/Cas9 technique, resulting in a *nth2 1271\_1272delTA* phenotypically normal strain that could grow under osmotic stress (0.85 M sodium chloride).

**Supplementary Materials:** The following supporting information can be downloaded at: <https://www.mdpi.com/article/10.3390/fermentation8040166/s1>, Figure S1: TEM images of the CEN.PK2-1C wild-type strain and mutated  $\Delta nth2$  strain of *S. cerevisiae* grown in 0 M and 0.85 M NaCl. The scale bar represents 0.5  $\mu\text{m}$  in all cases (5000 $\times$  magnification). N: nucleus, V: vacuole, M: mitochondrion, CM: cell membrane, CW: cell wall.; Figure S2. DNA alignment of the sequences of the *NTH1* and *NTH2* genes, including the gRNA position and primers used in this study. sgNTH1 = single guide *NTH1*, sgNTH2 = single guide *NTH2*, nth1f = forward *NTH1* primer, nth2f = forward *NTH2* primer, nth1r = reverse *NTH1* primer, nth2r = reverse *NTH2* primer; Figure S3. Representation of the gRNA and scaffold. A. The bRA89 plasmid with the corresponding Bpl1 sites used for replacement of gRNA. B. The final *NTH2*-sgRNA with the scaffold. C. The final *NTH1* sgRNA with the scaffold.

**Author Contributions:** Conceptualization, A.H.-S., J.P.D.-N. and A.G.-A.; writing—original draft preparation, A.H.-S., J.P.D.-N., M.B.-A., S.A.P. and A.G.-A.; writing—review and editing, A.H.-S., J.P.D.-N., M.B.-A., S.A.P. and A.G.-A.; visualization, A.H.-S., J.P.D.-N., M.B.-A., S.A.P. and A.G.-A. All authors have read and agreed to the published version of the manuscript.

**Funding:** This research was financed by the Espacio de Estudios Avanzados de la Universidad de Costa Rica (Space for Advanced Studies at the University of Costa Rica), grant number 801-B7-294, UCREA.

**Institutional Review Board Statement:** Not applicable.

**Informed Consent Statement:** Not applicable.

**Data Availability Statement:** Not applicable.

**Acknowledgments:** This article is part of the Doctoral Thesis of the first author, Doctorado en Ciencia Naturales para el Desarrollo (DOCINADE), Instituto Tecnológico de Costa Rica (TEC), Universidad Nacional, Universidad Estatal a Distancia, Cartago, Costa Rica. We thank Fabián Echeverría-Beirute of DOCINADE-ITCR for the assistance in reviewing and editing the manuscript. We also thank Ethel Sánchez-Chacón for TEM sample preparation and the Laboratorio Institucional de Microscopía of Tecnológico de Costa Rica for ultramicrotome cuts.

**Conflicts of Interest:** The authors declare no conflict of interest.

## References

1. Zhang, X.; Zhang, Y.; Li, H. Regulation of trehalose, a typical stress protectant, on central metabolisms, cell growth and division of *Saccharomyces cerevisiae* CEN.PK113-7D. *Food Microbiol.* **2020**, *89*, 103459. [[CrossRef](#)] [[PubMed](#)]
2. Paul, M.J.; Gonzalez-Uriarte, A.; Griffiths, C.A.; Hassani-Pak, K. The Role of Trehalose 6-Phosphate in Crop Yield and Resilience. *Plant Physiol.* **2018**, *177*, 12–23. [[CrossRef](#)]
3. Fichtner, F.; Lunn, J.E. The Role of Trehalose 6-Phosphate (Tre6P) in Plant Metabolism and Development. *Annu. Rev. Plant Biol.* **2021**, *72*, 737–760. [[CrossRef](#)] [[PubMed](#)]
4. Cai, X.; Seitz, I.; Mu, W.; Zhang, T.; Stressler, T.; Fischer, L.; Jiang, B. Biotechnical production of trehalose through the trehalose synthase pathway: Current status and future prospects. *Appl. Microbiol. Biotechnol.* **2018**, *102*, 2965–2976. [[CrossRef](#)] [[PubMed](#)]
5. Rapoport, A.; Golovina, E.A.; Gervais, P.; Dupont, S.; Beney, L. Anhydrobiosis: Inside yeast cells. *Biotechnol. Adv.* **2019**, *37*, 51–67. [[CrossRef](#)]
6. Glatz, A.; Pilbat, A.-M.; Németh, G.L.; Vince-Kontár, K.; Jósavay, K.; Hunya, Á.; Udvardy, A.; Gombos, I.; Péter, M.; Balogh, G.; et al. Involvement of small heat shock proteins, trehalose, and lipids in the thermal stress management in *Schizosaccharomyces pombe*. *Cell Stress Chaperon* **2016**, *21*, 327–338. [[CrossRef](#)]
7. Dong, J.; Chen, D.; Wang, G.; Zhang, C.; Du, L.; Liu, S.; Zhao, Y.; Xiao, D. Improving freeze-tolerance of baker's yeast through seamless gene deletion of NTH1 and PUT1. *J. Ind. Microbiol. Biotechnol.* **2016**, *43*, 817–828. [[CrossRef](#)]
8. Tapia, H.; Koshland, D.E. Trehalose Is a Versatile and Long-Lived Chaperone for Desiccation Tolerance. *Curr. Biol.* **2014**, *24*, 2758–2766. [[CrossRef](#)]
9. Olsson, C.; Jansson, H.; Swenson, J. The Role of Trehalose for the Stabilization of Proteins. *J. Phys. Chem. B* **2016**, *120*, 4723–4731. [[CrossRef](#)]
10. Bosch, S.; De Beaufort, L.; Allard, M.; Mosser, M.; Heichette, C.; Chrétien, D.; Jegou, D.; Bach, J.-M. Trehalose prevents aggregation of exosomes and cryodamage. *Sci. Rep.* **2016**, *6*, 36162. [[CrossRef](#)]
11. Babazadeh, R.; Lahtvee, P.-J.; Adiels, C.B.; Goksör, M.; Nielsen, J.B.; Hohmann, S. The yeast osmotic stress response is carbon source dependent. *Sci. Rep.* **2017**, *7*, 990. [[CrossRef](#)] [[PubMed](#)]
12. Garre, E.; Matallana, E. The three trehalases Nth1p, Nth2p and Ath1p participate in the mobilization of intracellular trehalose required for recovery from saline stress in *Saccharomyces cerevisiae*. *Microbiology* **2009**, *155*, 3092–3099. [[CrossRef](#)] [[PubMed](#)]
13. Mahmud, S.A.; Nagahisa, K.; Hirasawa, T.; Yoshikawa, K.; Ashitani, K.; Shimizu, H. Effect of trehalose accumulation on response to saline stress in *Saccharomyces cerevisiae*. *Yeast* **2009**, *26*, 17–30. [[CrossRef](#)] [[PubMed](#)]
14. Nwaka, S.; Kopp, M.; Holzer, H. Expression and Function of the Trehalase Genes NTH1 and YBR0106 in *Saccharomyces cerevisiae*. *J. Biol. Chem.* **1995**, *270*, 10193–10198. [[CrossRef](#)] [[PubMed](#)]
15. Nwaka, S.; Holzer, H. Molecular Biology of Trehalose and the Trehalases in the Yeast *Saccharomyces cerevisiae*. *Prog. Nucleic Acid Res. Mol. Biol.* **1997**, *58*, 197–237. [[CrossRef](#)]
16. Gibney, P.A.; Schieler, A.; Chen, J.C.; Rabinowitz, J.D.; Botstein, D. Characterizing the in vivo role of trehalose in *Saccharomyces cerevisiae* using the *AGT1* transporter. *Proc. Natl. Acad. Sci. USA* **2015**, *112*, 6116–6121. [[CrossRef](#)] [[PubMed](#)]
17. Hallerman, E.M.; Bredlau, J.P.; Camargo, L.S.A.; Dagli, M.L.Z.; Karambu, M.; Ngunjiri, G.; Romero-Aldemita, R.; Rocha-Salavarieta, P.J.; Tizard, M.; Walton, M.; et al. Towards progressive regulatory approaches for agricultural applications of animal biotechnology. *Transgenic Res.* **2022**, *3*, 1–33. [[CrossRef](#)]
18. Wang, P.-M.; Zheng, D.-Q.; Chi, X.-Q.; Li, O.; Qian, C.-D.; Liu, T.-Z.; Zhang, X.-Y.; Du, F.-G.; Sun, P.-Y.; Qu, A.-M.; et al. Relationship of trehalose accumulation with ethanol fermentation in industrial *Saccharomyces cerevisiae* yeast strains. *Bioresour. Technol.* **2014**, *152*, 371–376. [[CrossRef](#)]
19. Jules, M.; Beltran, G.; François, J.; Parrou, J.L. New Insights into Trehalose Metabolism by *Saccharomyces cerevisiae*: NTH2 Encodes a Functional Cytosolic Trehalase, and Deletion of TPS1 Reveals Ath1p-Dependent Trehalose Mobilization. *Appl. Environ. Microbiol.* **2008**, *74*, 605–614. [[CrossRef](#)]
20. Avila-Reyes, S.; Camacho-Diaz, B.; Acosta-Garcia, M.; Jimenez-Aparicio, A.; Hernandez-Sanchez, H. Effect of salt and sugar osmotic stress on the viability and morphology of *Saccharomyces boulardii*. *Int. J. Environ. Agric. Biotechnol.* **2016**, *1*, 593–602. [[CrossRef](#)]
21. Logothetis, S.; Walker, G.; Nerantzis, E. Effect of salt hyperosmotic stress on yeast cell viability. *Zb. Matic Srp. Prir. Nauk.* **2007**, *113*, 271–284. [[CrossRef](#)]
22. Divate, N.R.; Chen, G.-H.; Divate, R.D.; Ou, B.-R.; Chung, Y.-C. Metabolic engineering of *Saccharomyces cerevisiae* for improvement in stresses tolerance. *Bioengineered* **2017**, *8*, 524–535. [[CrossRef](#)] [[PubMed](#)]
23. Sun, X.; Zhang, C.-Y.; Wu, M.-Y.; Fan, Z.-H.; Liu, S.-N.; Zhu, W.-B.; Xiao, D.-G. MAL62 overexpression and NTH1 deletion enhance the freezing tolerance and fermentation capacity of the baker's yeast in lean dough. *Microb. Cell Factories* **2016**, *15*, 1–8. [[CrossRef](#)]
24. Nwaka, S.; Mechler, B.; Destruelle, M.; Holzer, H. Phenotypic features of trehalase mutants in *Saccharomyces cerevisiae*. *FEBS Lett.* **1995**, *360*, 286–290. [[CrossRef](#)]
25. Mahmud, S.A.; Hirasawa, T.; Shimizu, H. Differential importance of trehalose accumulation in *Saccharomyces cerevisiae* in response to various environmental stresses. *J. Biosci. Bioeng.* **2010**, *109*, 262–266. [[CrossRef](#)] [[PubMed](#)]
26. Tapia, H.; Young, L.; Fox, D.; Bertozzi, C.R.; Koshland, D. Increasing intracellular trehalose is sufficient to confer desiccation tolerance to *Saccharomyces cerevisiae*. *Proc. Natl. Acad. Sci. USA* **2015**, *112*, 6122–6127. [[CrossRef](#)] [[PubMed](#)]

27. Anand, R.; Beach, A.; Li, K.; Haber, J. Rad51-mediated double-strand break repair and mismatch correction of divergent substrates. *Nature* **2017**, *544*, 377–380. [[CrossRef](#)] [[PubMed](#)]
28. Naito, Y.; Hino, K.; Bono, H.; Ui-Tei, K. CRISPRdirect: Software for designing CRISPR/Cas guide RNA with reduced off-target sites. *Bioinformatics* **2015**, *31*, 1120–1123. [[CrossRef](#)]
29. Gietz, R.D.; Schiestl, R.H. High-efficiency yeast transformation using the LiAc/SS carrier DNA/PEG method. *Nat. Protoc.* **2007**, *2*, 31–34. [[CrossRef](#)]
30. Fernandez-Ricaud, L.; Warringer, J.; Ericson, E.; Pylvänäinen, I.; Kemp, G.J.L.; Nerman, O.; Blomberg, A. PROPHECY—a database for high-resolution phenomics. *Nucleic Acids Res.* **2004**, *33*, D369–D373. [[CrossRef](#)]
31. Doudna, J.A.; Charpentier, E. The new frontier of genome engineering with CRISPR-Cas9. *Science* **2014**, *346*, 1258096. [[CrossRef](#)] [[PubMed](#)]
32. Wang, H.; La Russa, M.; Qi, L.S. CRISPR/Cas9 in Genome Editing and Beyond. *Annu. Rev. Biochem.* **2016**, *85*, 227–264. [[CrossRef](#)] [[PubMed](#)]
33. Morris, G.J.; Winters, L.; Coulson, G.E.; Clarke, K.J. Effect of Osmotic Stress on the Ultrastructure and Viability of the Yeast *Saccharomyces cerevisiae*. *Microbiol.* **1986**, *132*, 2023–2034. [[CrossRef](#)] [[PubMed](#)]
34. Ewald, J.C.; Kuehne, A.; Zamboni, N.; Skotheim, J.M. The Yeast Cyclin-Dependent Kinase Routes Carbon Fluxes to Fuel Cell Cycle Progression. *Mol. Cell* **2016**, *62*, 532–545. [[CrossRef](#)]
35. Yi, C.; Wang, F.; Dong, S.; Li, H. Changes of trehalose content and expression of relative genes during the bioethanol fermentation by *Saccharomyces cerevisiae*. *Can. J. Microbiol.* **2016**, *62*, 827–835. [[CrossRef](#)]
36. Zähringer, H.; Burgert, M.; Holzer, H.; Nwaka, S. Neutral trehalase Nth1p of *Saccharomyces cerevisiae* encoded by the NTH1 gene is a multiple stress responsive protein. *FEBS Lett.* **1997**, *412*, 615–620. [[CrossRef](#)]
37. Iwahashi, H.; Nwaka, S.; Obuchi, K. Evidence for Contribution of Neutral Trehalase in Barotolerance of *Saccharomyces cerevisiae*. *Appl. Environ. Microbiol.* **2000**, *66*, 5182–5185. [[CrossRef](#)]
38. Singer, M.A.; Lindquist, S. Thermotolerance in *Saccharomyces cerevisiae*: The Yin and Yang of trehalose. *Trends Biotechnol.* **1998**, *16*, 460–468. [[CrossRef](#)]
39. Bravim, F.; Lippman, S.I.; da Silva, L.F.; Souza, D.T.; Fernandes, A.A.R.; Masuda, C.A.; Broach, J.R.; Fernandes, P.M.B. High hydrostatic pressure activates gene expression that leads to ethanol production enhancement in a *Saccharomyces cerevisiae* distillery strain. *Appl. Microbiol. Biotechnol.* **2013**, *97*, 2093–2107. [[CrossRef](#)]
40. Botts, M.R.; Huang, M.; Borchardt, R.K.; Hull, C.M. Developmental Cell Fate and Virulence Are Linked to Trehalose Homeostasis in *Cryptococcus neoformans*. *Eukaryot. Cell* **2014**, *13*, 1158–1168. [[CrossRef](#)]
41. Blevins, W.R.; Ruiz-Orera, J.; Messeguer, X.; Blasco-Moreno, B.; Villanueva-Cañas, J.L.; Espinar, L.; Díez, J.; Carey, L.B.; Albà, M.M. Uncovering de novo gene birth in yeast using deep transcriptomics. *Nat. Commun.* **2021**, *12*, 1–13. [[CrossRef](#)] [[PubMed](#)]
42. Cakiroglu, S.A.; Zaugg, J.B.; Luscombe, N.M. Backmasking in the yeast genome: Encoding overlapping information for protein-coding and RNA degradation. *Nucleic Acids Res.* **2016**, *44*, 8065–8072. [[CrossRef](#)]
43. Orr, M.W.; Mao, Y.; Storz, G.; Qian, S.-B. Alternative ORFs and small ORFs: Shedding light on the dark proteome. *Nucleic Acids Res.* **2020**, *48*, 1029–1042. [[CrossRef](#)] [[PubMed](#)]
44. Saini, P.; Beniwal, A.; Kokkiligadda, A.; Vij, S. Response and tolerance of yeast to changing environmental stress during ethanol fermentation. *Process Biochem.* **2018**, *72*, 1–12. [[CrossRef](#)]
45. Pratt, P.L.; Bryce, J.H.; Stewart, G.G. The Effects of Osmotic Pressure and Ethanol on Yeast Viability and Morphology. *J. Inst. Brew.* **2003**, *109*, 218–228. [[CrossRef](#)]
46. Muysson, J.; Miller, L.; Allie, R.; Inglis, D.L. The Use of CRISPR-Cas9 Genome Editing to Determine the Importance of Glycerol Uptake in Wine Yeast During Icewine Fermentation. *Fermentation* **2019**, *5*, 93. [[CrossRef](#)]
47. Vilela, A. An Overview of CRISPR-Based Technologies in Wine Yeasts to Improve Wine Flavor and Safety. *Fermentation* **2021**, *7*, 5. [[CrossRef](#)]